AD-A094 834 NAVAL RESEARCH LAB WASHINGTON DC F/G 20/1
THE DESIGN AND ANALYSIS OF A UNIQUE BROADBAND UNDERWATER ACOUST--ETC(U)
JAN 81 A M YOUNG
UNCLASSIFIED NRL-8435 NL

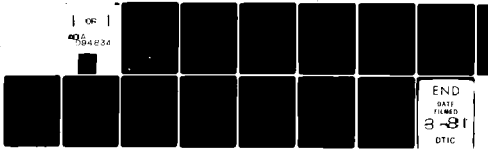

NRL Report 8435

The Design and Analysis of a Unique Broadband Underwater Acoustic Source

A. MARK YOUNG

Transducer Branch
Underwater Sound Reference Detachment
P.O. Box 8337
Orlando, FL 32856

January 13, 1981

NAVAL RESEARCH LABORATORY
Washington, D.C.

SECURITY CLASSIFICATION OF THIS PAGE (When Data Entered)

REPORT DOCUMENTATION PAGE	READ INSTRUCTIONS BEFORE COMPLETING FORM
1. REPORT NUMBER: NRL Report 8435 — 2. GOVT ACCESSION NO.: AD A094 834	3. RECIPIENT'S CATALOG NUMBER
4. TITLE (and Subtitle): THE DESIGN AND ANALYSIS OF A UNIQUE BROADBAND UNDERWATER ACOUSTIC SOURCE	5. TYPE OF REPORT & PERIOD COVERED: Interim report on a continuing NRL problem.
	6. PERFORMING ORG. REPORT NUMBER
7. AUTHOR(s): A. Mark Young	8. CONTRACT OR GRANT NUMBER(s)
9. PERFORMING ORGANIZATION NAME AND ADDRESS: Naval Research Laboratory, Underwater Sound Reference Detachment, P.O. Box 8337, Orlando, FL 32856	10. PROGRAM ELEMENT, PROJECT, TASK AREA & WORK UNIT NUMBERS: NRL Problems S02-36 & S99-01*
11. CONTROLLING OFFICE NAME AND ADDRESS: ONR/NRL Code 8000 (now 5000) and NAVSEA	12. REPORT DATE: January 16, 1981
	13. NUMBER OF PAGES: 18
14. MONITORING AGENCY NAME & ADDRESS (if different from Controlling Office)	15. SECURITY CLASS. (of this report): UNCLASSIFIED
	15a. DECLASSIFICATION/DOWNGRADING SCHEDULE

16. DISTRIBUTION STATEMENT (of this Report)

Approved for public release; distribution unlimited.

17. DISTRIBUTION STATEMENT (of the abstract entered in Block 20, if different from Report)

18. SUPPLEMENTARY NOTES

*Work was done under NRL Problems S02-36.401 and S99-01.101 prior to FY80. Funding for publication of this report will come from NRL Problems S200-0 (FY81) & 0583-0 (FY80). Portions of the work were previously reported in the author's M.S. thesis submitted to Florida Tech. Univ., Orlando in 1978.

19. KEY WORDS (Continue on reverse side if necessary and identify by block number)

Linear arrays
Directivity
Amplitude shading
Phase shading

20. ABSTRACT (Continue on reverse side if necessary and identify by block number)

The design, development, and analysis of a unique type of underwater acoustic source are discussed. The transducer is in the form of a linear array of discrete elements and is required to have a constant transmitting voltage response and carefully controlled directivity characteristics over a two-octave bandwidth. A generalized model of linear array of cylindrical piezoelectric ceramic acoustic radiators is developed and applied to the design of a prototype which operates over approximately half of the required bandwidth. The prototype transducer was built, and the measured results are compared with those predicted by the model. Recommendations are made for improving the performance of both the prototype and the array required to meet the full specified bandwidth.

DD FORM 1 JAN 73 1473 EDITION OF 1 NOV 65 IS OBSOLETE
S/N 0102-014-6601

SECURITY CLASSIFICATION OF THIS PAGE (When Data Entered)

CONTENTS

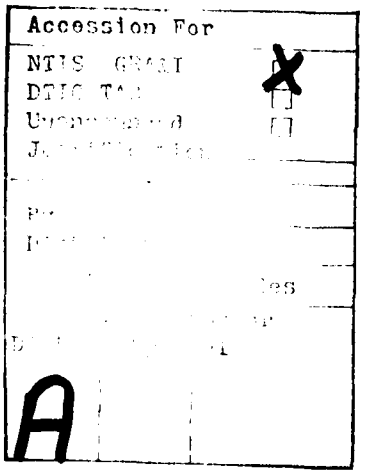

THE DESIGN AND ANALYSIS OF A UNIQUE BROADBAND UNDERWATER ACOUSTIC SOURCE

INTRODUCTION

Underwater electroacoustic calibration measurements taken in open bodies of water are typically made at relatively shallow depths. To minimize the multipath effects of reflections from the surface and bottom, it is often desirable to use a calibration source that discriminates against those directions over the frequency range of interest; that is, a source that essentially confines the radiation within a relatively narrow beam in the vertical plane. Calibration measurements can also be simplified if the output of the source is constant over the frequency range in which it will be used. However, this report shows that these two requirements are, in general, contradictory.

REQUIREMENTS

Directivity is typically the most difficult parameter to control over a wide frequency range. The intended application for this transducer requires a toroidal beam pattern; that is, omnidirectional in the horizontal plane with a main beamwidth between 30 to 60° (at the 3-dB down points) in the vertical plane. The sidelobes are required to be a minimum of 15 dB below the maximum level of the main beam. The directivity requirements are summarized in Fig. 1.

The directivity requirements of the subject transducer determine its basic geometrical configuration. The requirements for omnidirectionality in one plane and a specified

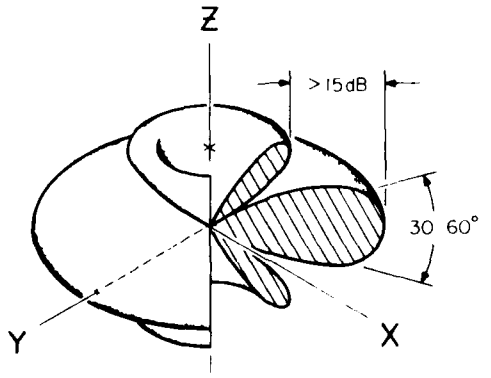

Fig. 1 — Summary of the directivity requirements

Manuscript submitted September 9, 1980.

beamwidth in a perpendicular plane imply the geometry of a linear array with the longitudinal array axis perpendicular to the omnidirectional plane. Also implied by the omnidirectionality in the horizontal plane is the cylindrical symmetry of the individual radiating elements. Therefore, based upon the directivity requirements, it can be assumed that the subject transducer will be in the basic form of a linear array of radially poled cylindrical piezoelectric ceramic shells.

The system incorporating the subject transducer requires an output sound pressure level (SPL) of 190 dB (referenced to 1 μPa measured at 1 m) over the frequency range from 10 to 40 kHz. It is required that the transmitting voltage response (TVR) be constant ($\pm$1.5 dB) over the same frequency range. The typical TVR of a piezoelectric ceramic cylindrical shell with the ends and inner surface acoustically shielded (or a linear array of such elements) is not flat, but instead has a +12 dB per octave slope at frequencies well below the frequency of the first radial resonance. Obviously then, a simple linear array of cylindrical elements will not meet the TVR requirements.

The requirement for the flat response demands that the distribution of the volume velocity generated by the array be such that the sum of the pressures in the far-field is a constant. This, coupled with the directivity requirements that the array length be a function of frequency, implies the biconical configuration shown in Fig. 2. The elements are arranged symmetrically with respect to the array center according to the frequency of their radial resonance; that is, the largest, lowest-frequency elements are at the ends of the array with the element size decreasing and the resonance frequency increasing symmetrically toward the array center. When the elements are driven electrically in parallel, the effective array length is a function of frequency with the array, in general, becoming shorter with increasing frequency.

In the succeeding sections, this report documents the development of a model of a generalized linear array of cylindrical acoustic radiators; the design, fabrication, and evaluation of a prototype of the subject transducer; and the comparison of the measured results with those predicted by the model.

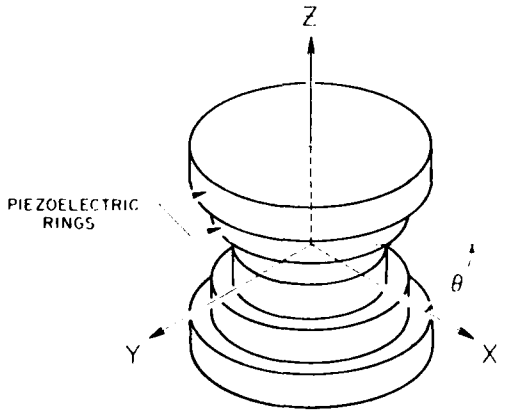

Fig. 2 — The biconical array configuration implied by the TVR and directivity requirements

ANALYSIS OF THE SUBJECT TRANSDUCER

In terms of what is already known about linear arrays, the desired transducer will be an unequally spaced, amplitude and phase-shaded linear array [1-6]. The elements will be unequally spaced primarily because of the requirement to tailor the volume velocity distribution to produce the flat TVR; that is, different element lengths are required for each element pair based upon their radial resonance frequency. Since the elements are connected electrically in parallel, the same voltage amplitude is present across each of the elements independent of the frequency. The array will, however, be amplitude shaded for two reasons. First, at any one frequency there is a relative difference in element amplitude due to their different frequencies of radial resonance. Second, the "adjusted" volume velocity distribution necessary for the required TVR is, of course, a form of amplitude shading. It should be obvious that the amplitude shading required by the transmitting response and the directivity is not necessarily the same. In fact, the two requirements are for the most part contradictory. The array will be phase shaded because, for a given frequency, the response curves of the individual element pairs are at different points relative to their resonance frequencies; in other words, there is a phase difference between the surface velocities of the element pairs.

The biconical configuration is essential to the directivity requirement in that the array will appear to effectively shorten as a function of increasing frequency. The key, of course, is controlling the response of each element pair at frequencies above resonance. One simplifying alternative would be to electrically series tune each element pair to its frequency of radial resonance. However, to do so would severely limit the bandwidth obtained from each pair and would result in a requirement for many more closely spaced elements, both physically and in frequency. In such a configuration the very small-diameter, thin-walled cylinders required for the highest frequencies could not produce the required SPL.

The biconical configuration also results in a reverse shading or negative tapering of the array. For example, at the resonance frequency of the largest, lowest-frequency elements the amplitude is highest at the ends of the array and decreases toward the center. As might be expected, this condition leads to a narrower main beam and higher sidelobe levels [7]. This may be partially overcome by judiciously choosing the center-to-center spacing of the elements.

In summary, the primary design parameters (all of which are interrelated) are the effective array length (as a function of frequency); the center-to-center spacing of the element pairs; the radiating area of the individual element pairs; and, of course, the relative positions (in frequency) of the radial resonance frequencies of the elements.

ANALYSIS

For the sake of simplicity, consider first the case of the far-field pressure generated by an array of two point sources radiating in phase. The generated pressure will be of the form

$$P_{1,2}(\theta) = A_1 e^{i\theta_1} + A_2 e^{i\theta_2}, \tag{1}$$

where A_1 and A_2 are the respective pressure amplitudes and θ_1 and θ_2 represent the phase of the two points with respect to the geometrical center of the array. Looking only at the real pressure amplitude,

$$P_{1,2}(\theta) = \left[(A_1 \cos \theta_1 + A_2 \cos \theta_2)^2 + (A_1 \sin \theta_1 + A_2 \sin \theta_2)^2 \right]^{1/2} , \tag{2}$$

or

$$P_{1,2}^2(\theta) = A_1^2 + A_2^2 + 2A_1A_2 \cos (\theta_1 - \theta_2) , \tag{3}$$

where the argument of the cosine term $\theta_1 - \theta_2$ represents the total phase difference between the two points. From the geometry of Fig. 3, it is obvious that $\theta_1 = kx$ and $\theta_2 = -kx$, where $k = 2\pi/\lambda$ and λ is the acoustic wavelength in water. Thus it is a simple matter to solve for x to yield $\theta_1 = kd/2$ and $\theta_2 = (-kd/2) \sin \theta$.

If we now consider the two sources to be cylindrical elements of finite but unequal radii, the phase relationship between the two is shown in Fig. 4. Now the total phase difference between the sources due to their separation in space is $k(x - r)$, where x and r may be found from Fig. 4 to be $d \sin \theta$ and $(a_2 - a_1) \cos \theta$, respectively. If the driving function (the electrical signal) is applied to the two elements in parallel, another phase difference becomes apparent.

Since the elements do not have the same mean radii, their radial resonances will occur at different frequencies and their surface velocities will therefore differ in phase. If the phase of the surface velocity with respect to the driving function is ϕ_1 and ϕ_2, respectively, Eq. (3) for the square of the generated far-field pressure becomes

$$P_{1,2}^2(\theta) = A_1^2 + A_2^2 + 2A_1A_2 \cos \left\{ \theta_1 - \theta_2 - k \left[d \sin \theta - (a_2 - a_1) \cos \theta \right] \right\} . \tag{4}$$

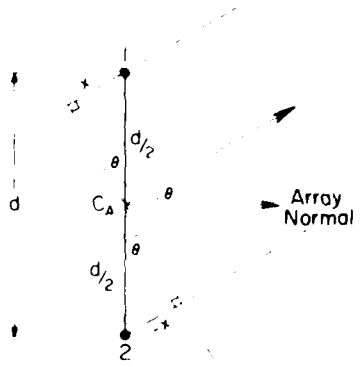

Fig. 3 — An array of two point sources separated by a distance d

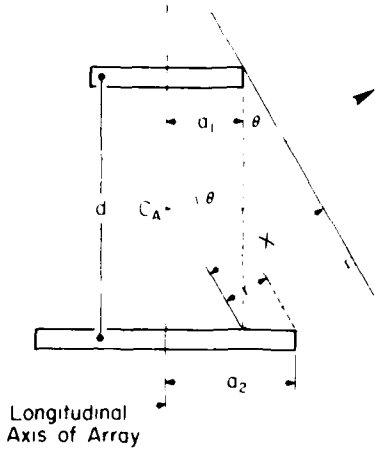

Fig. 4 -- An array of two cylindrical sources of unequal radii separated by a distance d

The square of the on-axis ($\theta = 0$) pressure reduces to

$$P_{1,2}^2(0) = A_1^2 + A_2^2 + 2A_1A_2 \cos\left[\phi_1 - \phi_2 + k(a_2 - a_1)\right] , \tag{5}$$

and the normalized directivity pattern becomes

$$\mathscr{P}_{1,2}(\theta) = \frac{P_{1,2}(\theta)}{P_{1,2}(0)} = \left\{ \frac{A_1^2 + A_2^2 + 2A_1A_2 \cos(\phi_1 - \phi_2 - \psi_{1,2})}{A_1^2 + A_2^2 + 2A_1A_2 \cos\left[\phi_1 - \phi_2 + k(a_2 - a_1)\right]} \right\}^{1/2} , \tag{6}$$

where $\psi_{1,2} = k\left[d \sin\theta - (a_2 - a_1)\cos\theta\right]$.

The elements are now of finite dimensions and can no longer be considered as point sources; that is, there is a nonunity directivity factor associated with each element. The pressure amplitudes of the individual elements as a function of θ now can be represented by $B_1 = A_1\left[\sin(k\ell_1/2 \cdot \sin\theta)/(k\ell_1/2 \cdot \sin\theta)\right]$ and $B_2 = A_2\left[\sin(k\ell_2/2 \cdot \sin\theta)/(k\ell_2/2 \cdot \sin\theta)\right]$ where the right-hand term in each expression is the normalized directivity pattern for a continuous line source of length ℓ_1 and ℓ_2, respectively. This can be shown to be simply an application of the product theorem [8], which (as applied to this case) states that if the point sources in the two-element array are replaced by finite sources, then the resulting directivity pattern for the array will be the product of the directivity patterns of the finite elements and the two-element point source array. To illustrate, Eq. (6) may be rewritten as

$$\mathscr{P}_{1,2}(\theta) = \left\{ \frac{B_1^2 + B_2^2 + 2B_1B_2 \cos(\phi_1 - \phi_2 - \psi_{1,2})}{A_1^2 + A_2^2 + 2A_1A_2 \cos\left[\phi_1 - \phi_2 + k(a_2 - a_1)\right]} \right\}^{1/2} \tag{7}$$

and if the elements are of equal size, Eq. (7) then reduces to

$$\mathscr{P}_{1,2}(\theta) = \frac{\sin\left[\frac{k\ell}{2}\sin\theta\right]}{\left[\frac{k\ell}{2}\sin\theta\right]} \cdot \frac{\sin\left[kd\sin\theta\right]}{2\sin\left[\frac{kd}{2}\sin\theta\right]}, \tag{8}$$

which is the product of the directivity patterns of a continuous line element of length ℓ with that of an array of two point sources separated by a distance d.

This overall approach may be generalized to include N arbitrarily dimensioned and spaced finite elements, and Eq. (4) may be written as

$$P_N^2(\theta) = \sum_{n=1}^{N}\sum_{m=1}^{N} B_n B_m \cos(\phi_n - \phi_m - \psi_{n,m}), \tag{9}$$

where $B_n = A_n \sin(k\ell_n/2 \cdot \sin\theta)/(k\ell_n/2 \cdot \sin\theta)$,
$B_m = A_m \sin(k\ell_m/2 \cdot \sin\theta)/(k\ell_m/2 \sin\theta)$,
$\psi_{n,m} = k\left[d_{n,m}\sin\theta - (a_m - a_n)\cos\theta\right]$, and
$d_{n,m}$ (or $d_{m,n}$) is the spacing between the nth and mth elements.

In generalized form, the square of the on-axis pressure is written as

$$P_N^2(0) = \sum_{n=1}^{N}\sum_{m=1}^{N} A_n A_m \cos\left[\phi_n - \phi_m + k(a_m - a_n)\right], \tag{10}$$

and the directivity pattern becomes

$$\mathscr{P}_N(\theta) = \left\{\frac{\sum_{n=1}^{N}\sum_{m=1}^{N} B_n B_m \cos(\phi_n - \phi_m - \psi_{n,m})}{\sum_{n=1}^{N}\sum_{m=1}^{N} A_n A_m \cos\left[\phi_n - \phi_m + k(a_m - a_n)\right]}\right\}^{1/2}. \tag{11}$$

Before these expressions can be used to compute the TVR or the directivity patterns in the vertical plane, the pressure amplitudes (the A coefficients) for the individual cylindrical elements must be determined. In general, the far-field pressure from each element can be represented by [9]

$$P = \left\{\frac{U^2 R_A R_\theta \rho_0 c}{4\pi r^2}\right\}^{1/2}, \tag{12}$$

where U is the root-mean-square (rms) volume velocity of the radiator, R_A is the acoustic resistance acting on the radiator, R_θ is the directivity factor, $\rho_0 c$ is the characteristic impedance of the medium, and r is the distance to the measurement point. The diffraction constant for such a source may be written as [9]

$$D = \left(\frac{R_A R_\theta 4\pi}{k^2 \rho_0 c} \right)^{1/2} , \tag{13}$$

which may be solved for R_θ and substituted into Eq. (12). With this substitution, the expression for the pressure becomes

$$P = \frac{UDk\rho_0 c}{4\pi r} . \tag{14}$$

Using the definition of the volume velocity ($U = u \cdot S$) and the surface area of the cylinder ($S = 2\pi a \ell$), the pressure may be expressed as

$$P = \frac{u\rho_0 cDka\ell}{2r} , \tag{15}$$

where u is the rms velocity of the radiating surface, a is the radius of the cylinder, and ℓ is the cylinder's length. Now it is only necessary to find an expression for the surface velocity in order to compute the far-field pressure produced by each element.

The radial velocity of the cylindrical elements will be of the form

$$v = u \cos(\omega t - \phi) , \tag{16}$$

where the velocity amplitude u is the ratio of the rms force to the mechanical impedance of the ceramic cylinder and ϕ is the phase difference between the driving function and velocity. The mechanical impedance and phase angle are defined conventionally as $Z_m = R_m + jX_m$ and $\phi = \tan^{-1}(X_m / R_m)$ where R_m and X_m are the mechanical resistance and reactance, respectively. By using the definition of the mechanical quality factor Q and the fact that

$$X_m = \omega M - \frac{1}{\omega C_m} ,$$

the magnitude of the impedance is found to be

$$|Z_m| = \frac{\left[\frac{\omega^2}{\omega_0^2} + Q^2 \left(\frac{\omega^2}{\omega_0^2} - 1 \right)^2 \right]^{1/2}}{\omega C_m Q} , \tag{17}$$

where M and C_m are the mass and mechanical compliance, ω is the frequency in radians per second, ω_0 is the radial resonance frequency in radians per second, and $Q = 1/\omega_0 R_m C_m$. Similarly, the phase angle can be found to be

$$\phi = \tan^{-1}\left\{\frac{Q\left(\frac{\omega^2}{\omega_0^2} - 1\right)}{\frac{\omega}{\omega_0}}\right\} . \tag{18}$$

The rms force produced by the piezoelectric ceramic is given by

$$F = \frac{2\pi \ell d_{31} V}{S_{11}^E} . \tag{19}$$

d_{31} is the piezoelectric strain constant, where the subscripts denote the axes of the applied electric field and induced strain respectively, S_{11}^E is the reciprocal elastic modulus at constant electric field (S_{11}^E is the reciprocal of Young's modulus), and V is the rms value of the applied voltage. If we now take the ratio of the magnitude of the force to the magnitude of the mechanical impedance, we get

$$|u| = \frac{2\pi \ell d_{31} V \omega C_m Q}{S_{11}^E \left(\frac{\omega^2}{\omega_0^2} + Q^2\left(\frac{\omega^2}{\omega_0^2} - 1\right)^2\right)^{1/2}} \tag{20}$$

for the magnitude of the velocity. Substituting $C_m = aS_{11}^E 2\pi\ell$ [10] and $R_m = \rho_0 c(2\pi a\ell)$ along with the above expression and the expression for tan ϕ into Eq. (15) and performing the algebraic manipulation, we obtain

$$|P| = \frac{d_{31} V (\rho / S_{11}^E)^{1/2} Da\ell\omega\omega_0 \cos\phi}{2rc} \tag{21}$$

for the pressure generated by the individual elements (where ρ is the density of the piezoelectric ceramic). Equation (21) may be substituted into Eq. (9) for the A coefficients

and both sides of the result divided by V^2 to yield the far-field pressure per volt from the generalized array. The result is

$$\left|\frac{P_N(\theta)}{V}\right| = \frac{\omega d_{31}(\rho/S_{11}^E)^{1/2}}{2rc} \times \left\{ \sum_{n=1}^{N} \sum_{m=1}^{N} \frac{K_n \sin u_n}{u_n} \frac{K_m \sin u_m}{u_m} \cos(\phi_n - \phi_m - \psi_{n,m}) \right\}^{1/2}, \quad (22)$$

where $K_n = D_n a_n \ell_n \omega_n \cos\phi_n$, $K_m = D_m a_m \ell_m \omega_m \cos\phi_m$, $u_n = (k\ell_n/2)\sin\theta$, and $u_m = (k\ell_m/2)\sin\theta$. The on-axis sum of the pressures per volt (the TVR) reduces to

$$\left|\frac{P_N(0)}{V}\right| = \frac{\omega d_{31}(\rho/S_{11}^E)^{1/2}}{2rc} \left\{ \sum_{n=1}^{N} \sum_{m=1}^{N} K_n K_m \cos\left[\phi_n - \phi_m + k(a_m - a_n)\right] \right\}^{1/2}, \quad (23)$$

and the directivity pattern of the N-element line array becomes

$$\mathscr{P}_N(\theta) = \left\{ \frac{\sum_{n=1}^{N} \sum_{m=1}^{N} \frac{K_n \sin u_n}{u_n} \frac{K_m \sin u_m}{u_m} \cos(\phi_n - \phi_m - \psi_{n,m})}{\sum_{n=1}^{N} \sum_{m=1}^{N} K_n K_m \cos\left[\phi_n - \phi_m + k(a_m - a_n)\right]} \right\}^{1/2}. \quad (24)$$

The cylindrical elements have been assumed to vibrate only in the radial mode, and the mutual effects between radiating elements have been neglected, or at least to this point lumped into one unknown parameter—the diffraction constant.

If the mutual coupling effects between elements are ignored, the precise diffraction constant for the biconical configuration is still unknown and would be extremely difficult to determine. However, expressions do exist for the diffraction constants of a thin cylindrical ring and a long cylinder. By direct integration, Henriquez [11] found the diffraction constants for these two configurations to be

$$D_{\text{ring}} = J_0(ka) \quad (25)$$

and

$$D_{\text{cylinder}} = \frac{2}{\pi ka}\left[J_1^2(ka) + N_1^2(ka)\right]^{-1/2}, \quad (26)$$

where J_0 and J_1 are the zeroth and first order Bessel functions and N_1 is the first order Neumann function. Considered individually, the array elements are probably best described as thin rings. In the array, however, adjacent elements act as a tapered cylindrical baffle (at least geometrically) and the long cylinder configuration is perhaps more descriptive. Equation (26) will be used as an approximation to the diffraction constants of the array elements in Eqs. (23) and (24).

A program was written to carry out the calculations indicated in Eqs. (23) and (24) on a PDP-11/45 digital computer. Data input is required to specify the piezoelectric material type (the piezoelectric constant, the reciprocal elastic modulus, and the material density), the element dimensions (outside diameter, wall thickness, and length), and the center-to-center spacing of the elements in the array. There is the option of selecting the program output as either the TVR over a specified frequency range or the directivity patterns at specified discrete frequencies. The data may be displayed in tabulated form on a terminal or plotted on an X-Y plotter.

THE PROTOTYPE ARRAY

To provide a relatively simple first test of the model, a prototype array was designed to operate over approximately half of the total required bandwidth. The array contains four elements (two element pairs) and operates from 15 to 30 kHz. An iterative procedure using the computer program to compute the TVR was utilized to determine the element sizes. The element diameters and wall thicknesses were varied within the constraints of available ceramic sizes and the lengths varied to obtain the desired flatness of response. While maintaining the same ratio of element lengths and remaining within the constraints of the required SPL and electroacoustic efficiency, the elements were then shortened in order to minimize the element spacing in the array. Using this procedure, the array shown in Fig. 5

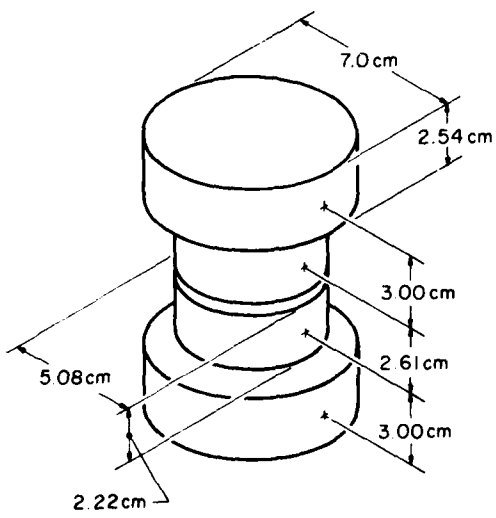

Fig. 5 — Dimensions of the prototype array for the frequency range from 15 to 30 kHz

was derived. The center-to-center spacing of the elements is not simply one half of the sum of the lengths of adjacent elements, because of the space occupied by mounting hardware.

The generalized model describes an array where the elements are radially vibrating cylindrical radiators free from any mechanical or acoustical coupling effects. We have already chosen to ignore any mutual acoustical effects to simplify the analysis, but care must be taken in the design to assure that the elements are not mechanically coupled through the mounting structure. To mechanically decouple each element from its mounting, glass-loaded polycarbonate end rings are fastened to each end of the ceramic cylinders with a thin film of relatively compliant potting compound. Since the elements are to be air backed, the end rings seal against a center mounting spindle by using elastomer O-ring seals. The spindles are in turn mounted to a single central shaft in the transducer by a cast ring of compliant potting compound. A single element and its mounting configuration are shown in Fig. 6.

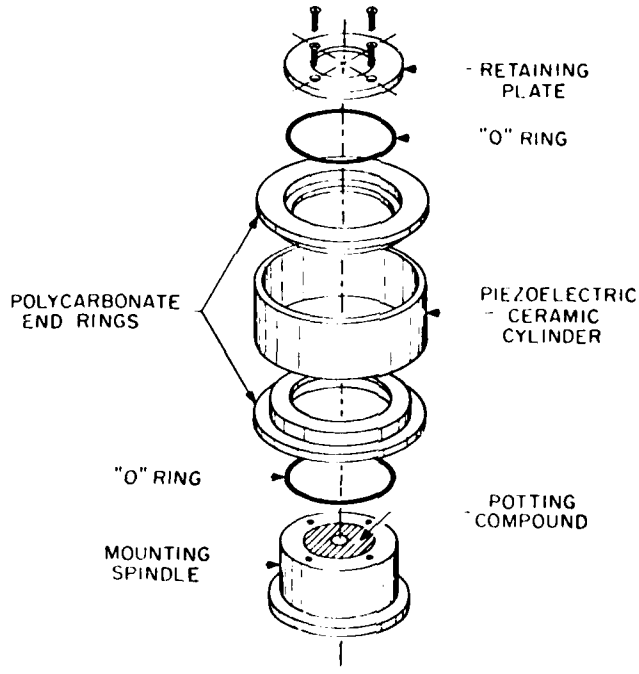

Fig. 6 -- An exploded view of a single prototype element and its mounting structure

Cylindrical stainless steel end plates are fastened to each end of the central mounting shaft, and the transducer is sealed in an elastomer cylindrical boot and filled with castor oil. The complete transducer is shown in Fig. 7.

COMPARISON OF RESULTS

The acoustical characteristics of the prototype array were measured in the frequency range from 15 to 30 kHz and to hydrostatic pressures of 4 MPa. Measurements made included TVR, directivity patterns in the horizontal (XY) and vertical (XZ) planes, and the linearity of output SPL as a function of driving voltage. All of the measurements show very little change (less than 0.5 dB) as a function of hydrostatic pressure, and the horizontal directivity patterns are omnidirectional (±1.0 dB). The transducer is linear as a function of driving voltage within ±0.5 dB.

The array easily produces the required on-axis SPL. At an output SPL of 190 dB (reference to 1 μPa and measured at a distance of 1 m) the electric field on the smallest, thinnest-wall ceramic is 1000 V/cm, or approximately half of the voltage it can safely withstand.

The TVR as predicted by Eq. (23) is compared to the measured response in Fig. 8. The two response curves agree to within 1.5 dB or less and are flat (±1.5 dB) over the design frequency range of 15 to 30 kHz. The close agreement between the curves indicates that the

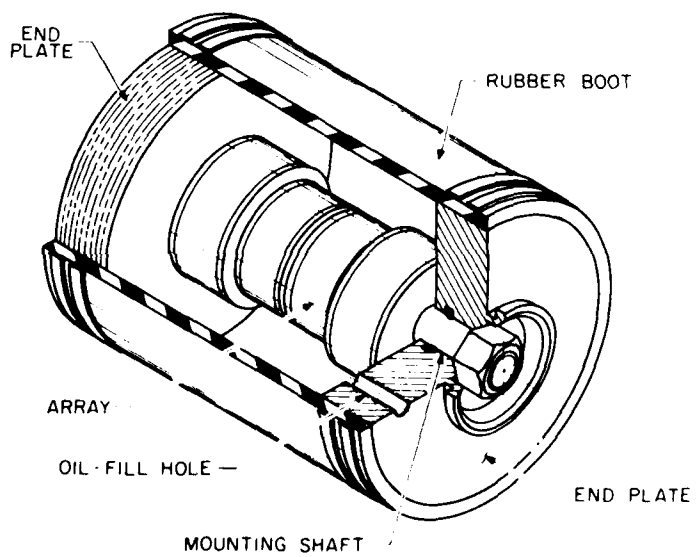

Fig. 7 — The assembled prototype transducer

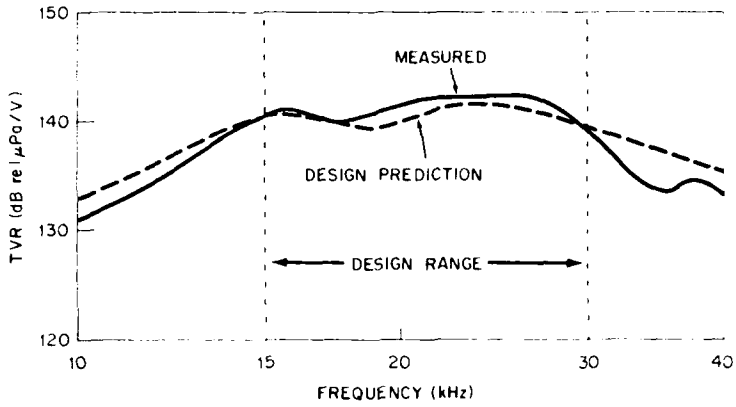

Fig. 8 — Comparison of the measured TVR of the prototype array with that predicted by the model

error introduced by neglecting mutual radiation effects between the elements is small, at least for the case of the prototype transducer.

The predicted (Eq. 24) vertical directivity patterns are compared to the measured patterns at 15, 20, and 30 kHz in Figs. 9 (a), (b), and (c) respectively. Only half of the full vertical patterns is shown in the figures because the other half is simply its mirror image. Some general conclusions can be reached about the measured patterns in terms of the specifications; the width of the main beam at the 3-dB down points is marginally acceptable but the sidelobe levels are too high, particularly at the lower frequencies. Some general observations may also be made about the accuracy of the model; while the width of the main beam is reasonably well predicted, the fine structure of the pattern (the nulls and sidelobe levels) is not. The prediction of the width of the main beam is reasonable, probably because the diffraction constant used (Eq. 26) and the normalized directivity pattern assumed for the individual elements in the model are accurate for the narrow angular confines of the main beam. As the observation point becomes further off the axis of the main beam, the unaccounted for effects form the adjacent elements and the housing end plates alter the effective diffraction constants and the normalized directivity patterns of the individual elements. This is probably best illustrated by examining the measured directivity pattern at 15 kHz. The sidelobes of the pattern look very similar to what one would expect from the larger two end elements spaced 0.8 λ apart; that is, the effect of the center elements is less than predicted by the model.

CONCLUSIONS

The directivity characteristics of the prototype array can be brought to within the specifications over the 15- to 30-kHz frequency range very easily; that is, the array can simply be shortened to an effective length of approximately $\lambda/2$. This is a feasible approach in the case of the prototype because we can reduce the ceramic volume by almost half and still maintain a safe driving voltage level. If the lengths of the element pairs are scaled from

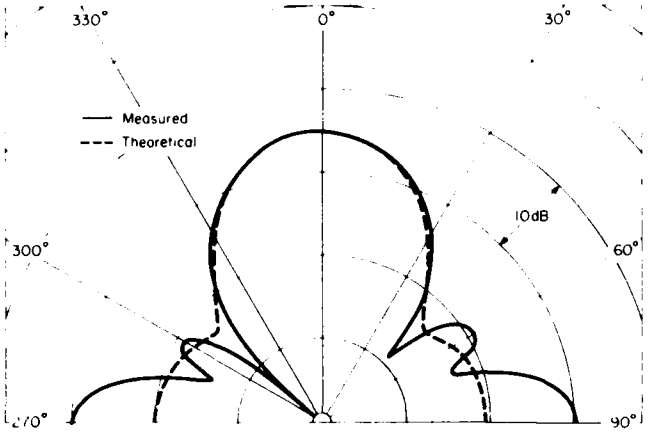

Fig. 9(a) — Comparison of the measured vertical (XZ) directivity pattern at 15 kHz with that predicted by the model

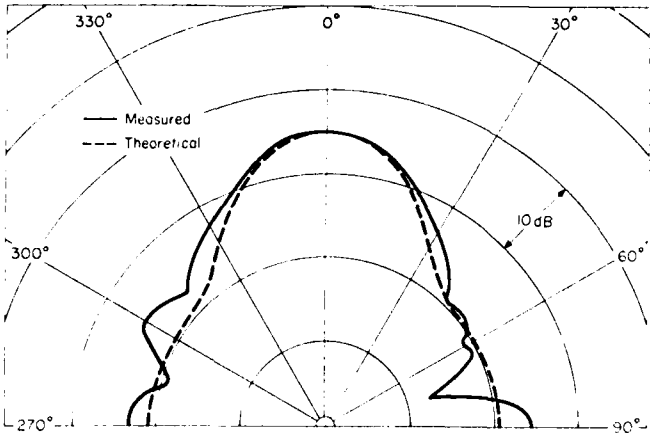

Fig. 9(b) — Comparison of the measured vertical (XZ) directivity pattern at 20 kHz with that predicted by the model

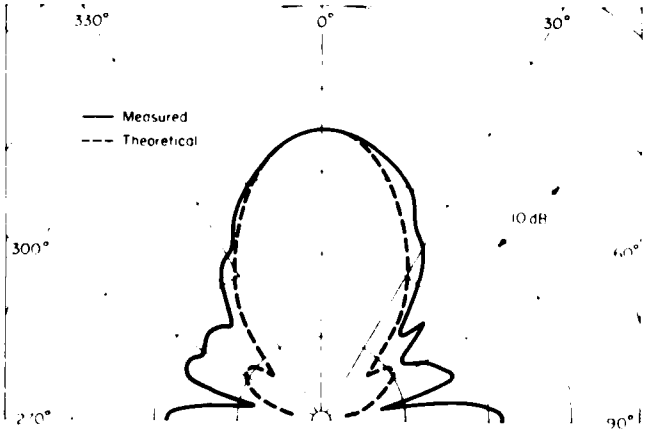

Fig. 9(c) — Comparison of the measured vertical (XZ) directivity pattern at 30 kHz with that predicted by the model

the present configuration, the flatness of the TVR will be maintained but the output level per volt will, of course, be lower. Reducing the volume of piezoelectric ceramic will also lower the electroacoustic efficiency although some of the loss may be regained by parallel tuning the array with the appropriate inductor.

Model predictions indicate that an array designed for the full required frequency range of 10 to 40 kHz will require eight elements (four element pairs). The safe driving voltage limit for such an array is determined by the addition of a higher frequency, even thinner walled pair of elements. Lowering the driving voltage limit has the effect of lengthening the lower frequency elements and therefore the total array. Obviously then, shortening the full array to a length of approximately $\lambda/2$, as recommended for the prototype, will probably not be feasible.

Another approach, however, does seem feasible for controlling the directivity characteristics of the full array. The requirements for the flat TVR and the broad main beam and low sidelobes are contradictory; that is, the flat response requires that the element amplitudes be greatest at the ends of the array and decrease toward the center, the beamwidth and sidelobe requirements imply just the opposite. If the response requirements are relaxed from flat to a positive slope as a function of increasing frequency (for example, +6 dB per octave), the directivity requirements can probably be met. This is true because adding a positive slope to the response is the same as applying a linear taper (linear shading) to the array. The output sound pressure from the array could still be made constant as a function of frequency by applying the reverse slope (-6 dB per octave) to the amplitude of the driving voltage. The computer model could still be used to determine the element sizes required for the desired slope and to optimize the array length in terms of the directivity and efficiency requirements. The positive slope approach will be addressed in future work.

REFERENCES

1. Vernon M. Albers, *Underwater Acoustics Handbook II* (The Pennsylvania State University Press, University Park, 1965).
2. Paul M. Kendig, "Directional Patterns of Transducer Arrays," Ordnance Research Laboratory Report No. NOrd 16597-7, University Park, Pa., ORL, 1956.
3. R. E. Collin and F. L. Zucker, *Antenna Theory* Part I (McGraw-Hill Book Co., New York, 1969).
4. L. Thourel, *The Antenna* (John Riley and Sons, Inc., New York, 1960).
5. C. L. Dolph, "A Current Distribution Which Optimizes the Relationship Between Beamwidth and Sidelobe Level," *Proc. Institute of Radio Engineers* 34, 335, June 1946.
6. C. L. Dolph, "Discussion on a Current Distribution Which Optimizes the Relationship Between Beamwidth and Sidelobe Level," *ibid.*, p. 492.
7. *Handbook of Array Design Technology* (Hydro-Acoustics Research, Inc., Washington, D.C., 1976), Vol. I.

8. H. Stenzel, *The Directional Characteristics of Radiators Arranged in a Plane* (Naval Research Laboratory Translation No. 114. Washington, D.C., NRL, 1947).

9. R. J. Bobber, "Diffraction Constants of Transducers," *J. Acoust. Soc. Am.* 37, 591, April 1965.

10. W. P. Mason, *Physical Acoustics* (Academic Press, New York, 1964), Vol. I, Part A.

11. T. A. Henriquez, "Diffraction Constants of Acoustic Transducers," *J. Acoust. Soc. Am.* 36, 267, February 1964.

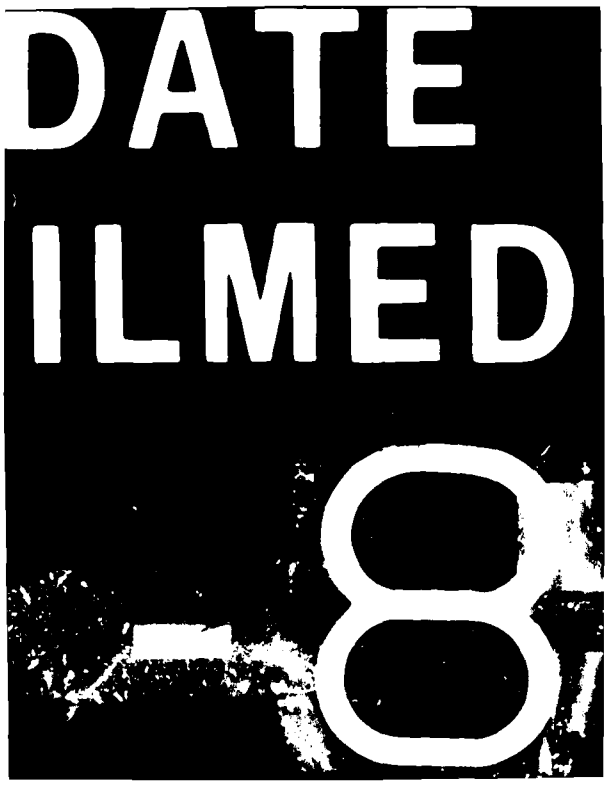
DATE
ILMED
8